

Charalambous C.¹, Baker M.², Golombek M.³, McClean JB.¹, Pike WT.¹, Spiga A.⁴, Lemmon M.⁵, Ansan V.⁶, Perrin C.⁷, Lorenz R.⁸, Weitz CM⁹, Grant J. A¹⁰, Warner NH.¹¹, Stott AE.¹, Murdoch N.¹², Rodriguez S.⁷, Banks M.E.¹³, Warren T.¹⁴, Johnson C.¹⁵, Mittelholz A.¹⁵, Hauber E.¹⁶, Daubar I.¹⁷, Navarro S.¹⁸, Sotomayor LM.¹⁸, Maki J.¹¹, Newman C.¹⁹, Viúdez-Moreiras D.¹⁸, Lucas A.¹², Banfield D.²⁰, Pla-García J.¹⁸, Lognonné P.¹², Banerdt WB.¹¹

¹ICL, UK (cc705@imperial.ac.uk), ²JHU, USA, ³JPL, Caltech, ⁴LMD, FR, ⁵SSI, USA, ⁶U. de Nantes, FR, ⁷IPGP, FR, ⁸APL, USA, ⁹PSI, USA, ¹⁰SI, USA, ¹¹SUNY Geneseo, USA, ¹²ISAE, FR, ¹³NASA GSFC, USA,, USA, ¹⁴OX, UK, ¹⁵UBC, CA, ¹⁶DLR, DE, ¹⁷Brown, USA, ¹⁸CAB, ES, ¹⁹AR, USA, ²⁰Cornell, USA

Introduction

Here, we present the most prominent aeolian in-situ changes by the lander during its first 400 sols of operations. Particle creep, dust removal and possibly saltation are for the first time complemented by simultaneous observations of high-cadence meteorological, seismological, and magnetic measurements on Mars. The observed changes exhibit seasonality and show a systematic association with the passage of convective vortices, inducing sudden peak winds that promote surface motion during sequences of enhanced vortex activity. These episodic aeolian changes, which consistently occur between noon to 3 pm local time, are correlated with excursions in both seismic and magnetic signals suggesting vortex-induced ground movement and charged-particle motion.

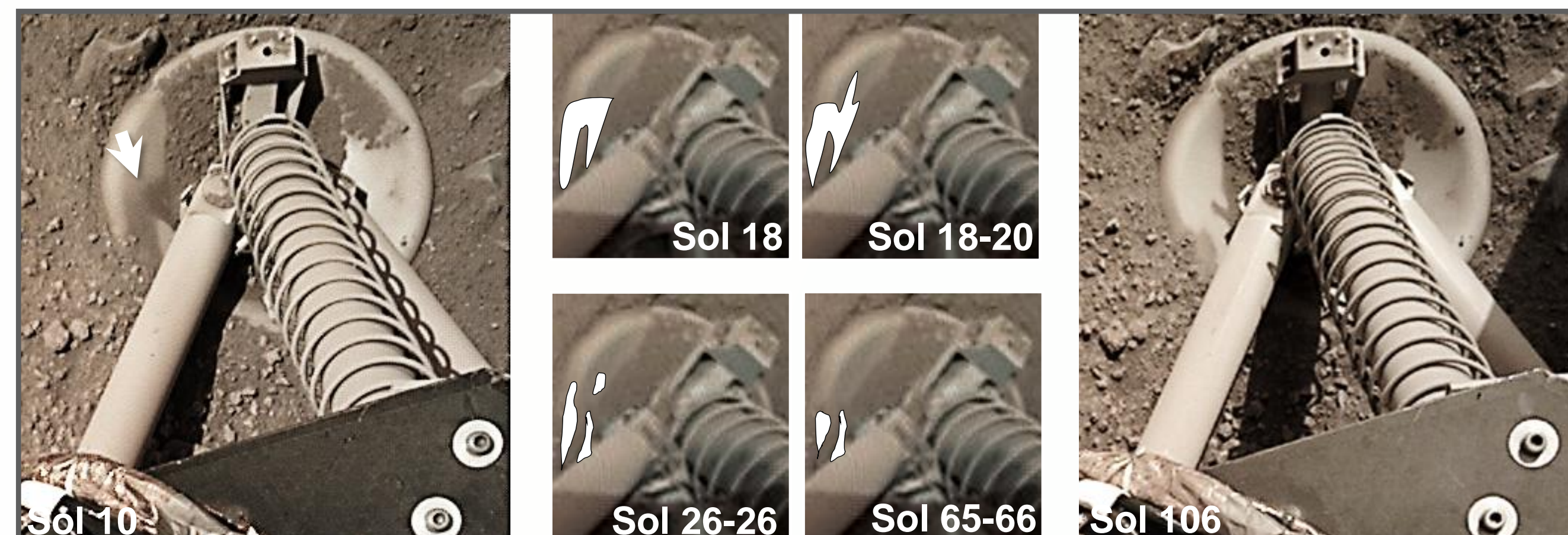
Method

Pairs of images taken under similar lighting conditions were compared by eye and image differencing, which allows more subtle changes to be identified. When available, a third image, ideally taken by the IDC, was used to confirm that an aeolian change had occurred. Once an aeolian change was identified, SEIS and APSS measurements were retrieved.

Aeolian Changes

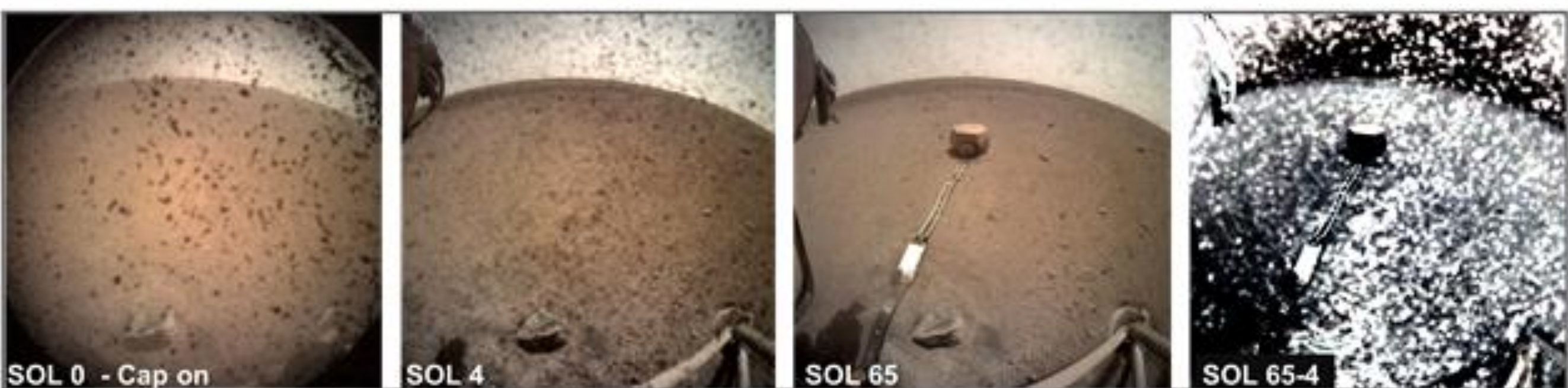
1. Removal of dust patch on west lander footpad

A patch of fine sediment patch was episodically removed on three sols (S): between image pairs of S18-S20, S26, and S65-S66 (Fig. 1a). There is evidence of transportation along the footpad in the first event, likely from the $\Delta P = 5.8$ Pa vortex on S19 and 23.8 ms^{-1} wind speed u_x , exhibiting an excursion in the magnetic signature and carving the first DD track observed at InSight by image differencing. The second removal occurred on S26 with $u_x = 28.2 \text{ ms}^{-1}$, and a $\Delta P = 4.1$ Pa vortex. The final change occurred on S65, after a $\Delta P = 9.2$ Pa inducing a $u_x = 20.1 \text{ ms}^{-1}$.



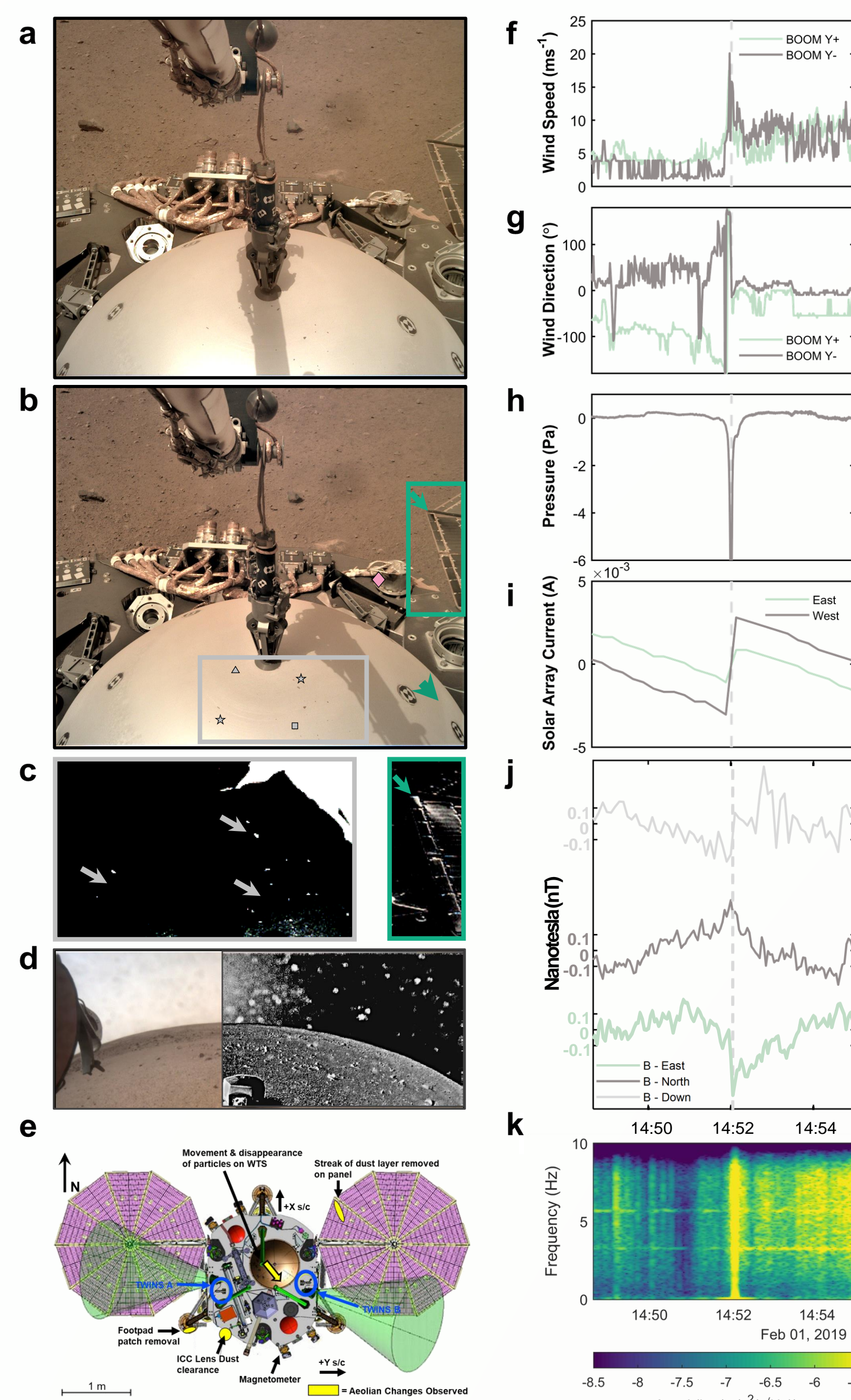
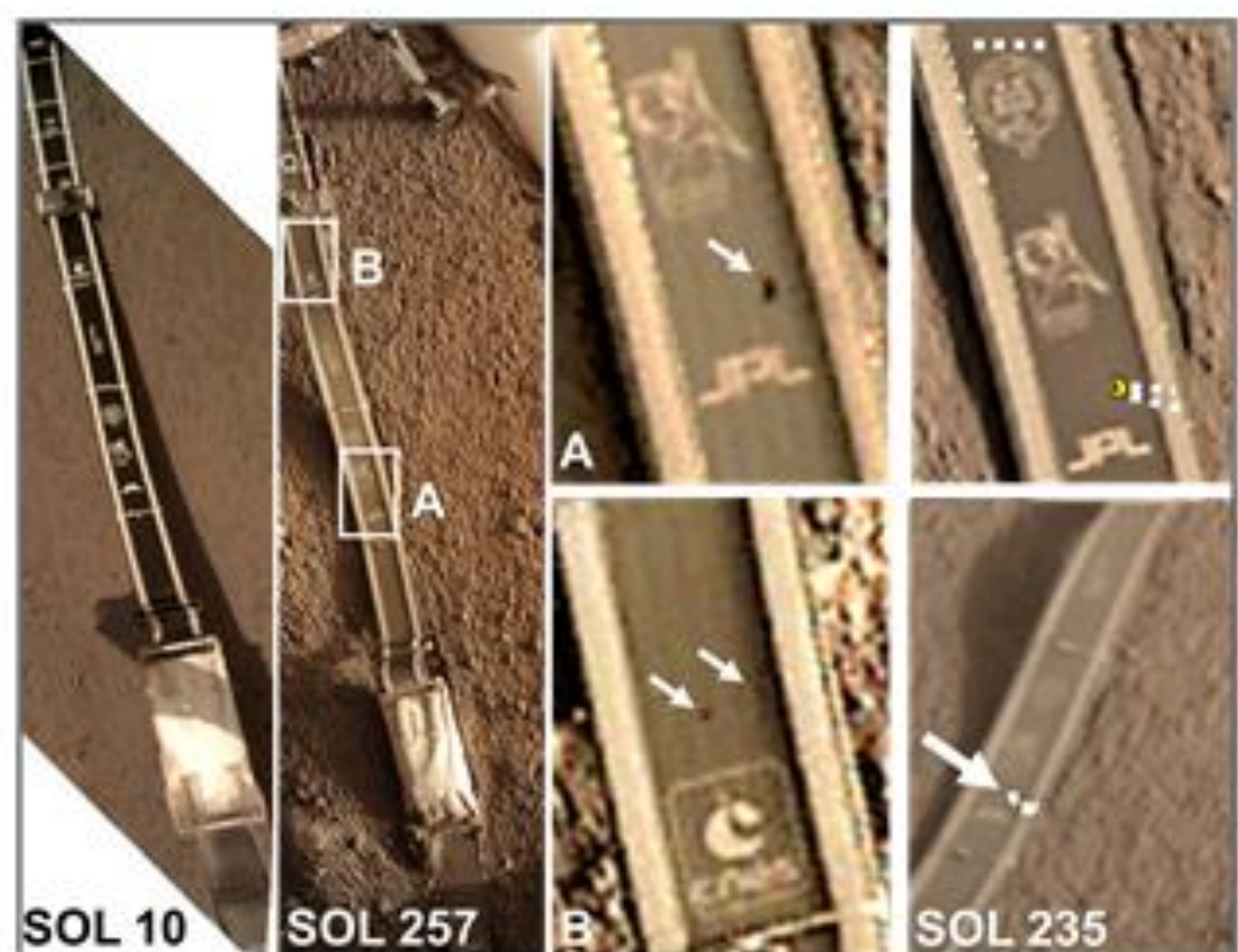
2. Changes on the ICC lens:

Significant ICC dust cleaning was observed during the first 66 sols. Matched peak speeds ranged from $15\text{--}28 \text{ ms}^{-1}$ with ΔP ranging from $0.8\text{--}9.2$ Pa, clustered at peak wind source directions of $\sim 140^\circ$ or $\sim 285^\circ$. This suggests dust was effectively removed when the wind impinged at a glancing angle.



3. Tether

A crescent-shaped dark spot ($0.5 \text{ cm} \times 0.25 \text{ cm}$) appeared on the SEIS tether on S235. Conical rays were seen extending to its right. IDC from S257 also shows two smaller dark spots of $d < 1 \text{ mm}$ and a fine, horizontal streak. The color is consistent to the tether's dust-free surface, while the shape and rays suggest an easterly trajectory, likely impacting and removing localized dust deposits. HiRISE image comparison between S218-S293 suggests a $\sim 10 \text{ m}$ wide DD track created 50 m to the east as a potential sourcing event.



4. Lander deck and solar arrays

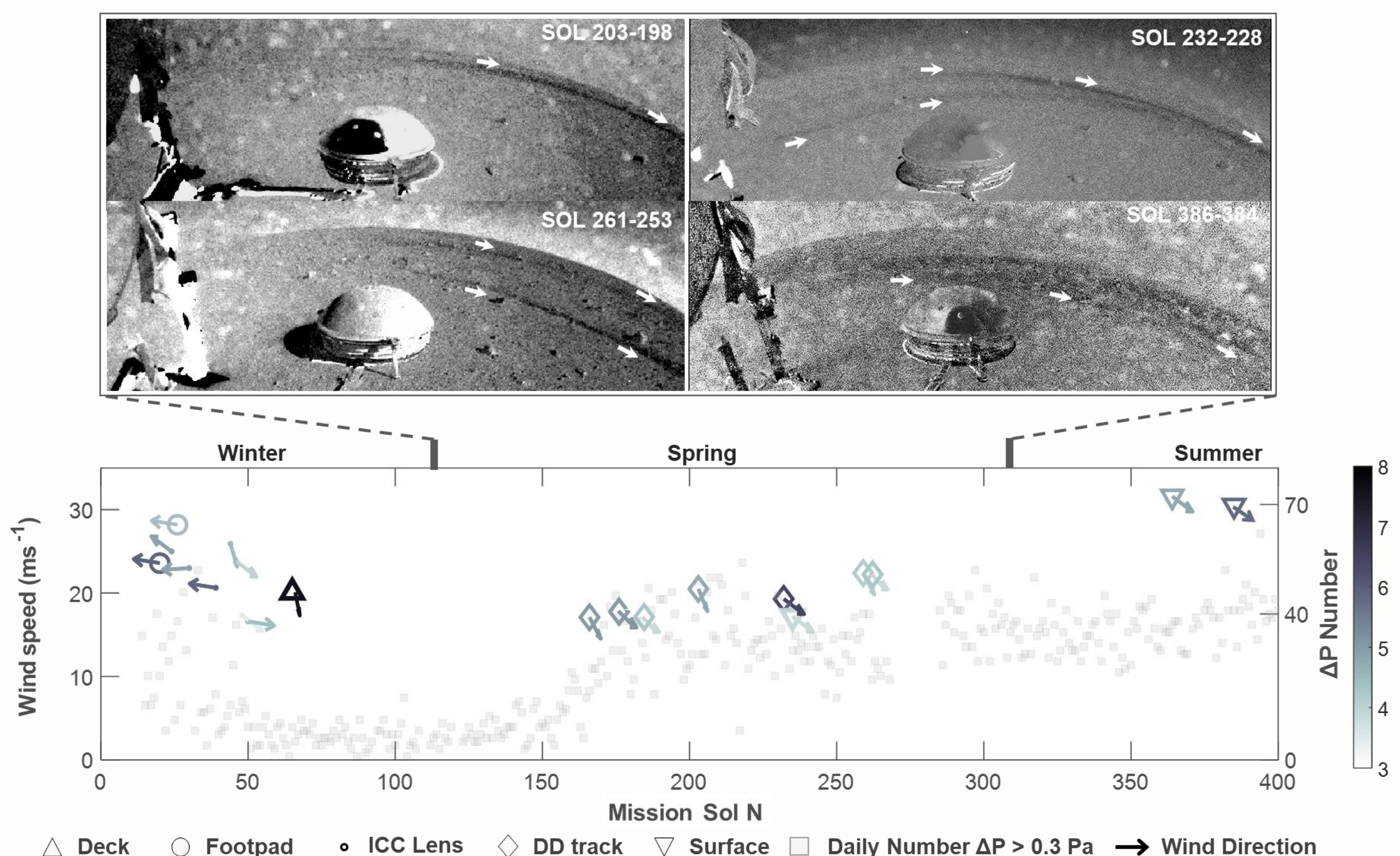
Aeolian changes on the lander were detected between IDC images taken on S65 at 13:25 and 14:24 LMST, six minutes after the occurrence of the deepest pressure drop recorded on Mars at $\Delta P = 9.2 \text{ Pa}$, associated with a wind speed of 20.1 ms^{-1} . Two notable changes were observed: particle motion on the Wind and Thermal Shield (WTS) and removal of a streak of dust in the lee of one of the ribs of the solar panels, illustrated in Fig.b,c. These changes likely happened simultaneously with the dust removal from the footpad (Fig. 1a).

Based on the shape, dark color and texture, and from at least one disaggregation example, these particles are likely dust aggregates (Greeley, 2002). Supporting this hypothesis, a particle, marked in square in Fig.b, appears disaggregated in the measured wind direction. Stars show at least four of the particles that moved in the measured wind direction. The triangle shows one example of disappearance, with the yellow diamond indicating motion of multiple grains on the deck.

5. Dust devil tracks

Numerous DD tracks were identified in differenced lander images implying dust entrainment. The DD tracks are consistently oriented in a consistent dominant wind direction, exhibit seasonality and cluster in the mid-spring season, in agreement with HiRISE observations (Perrin et al., 2020).

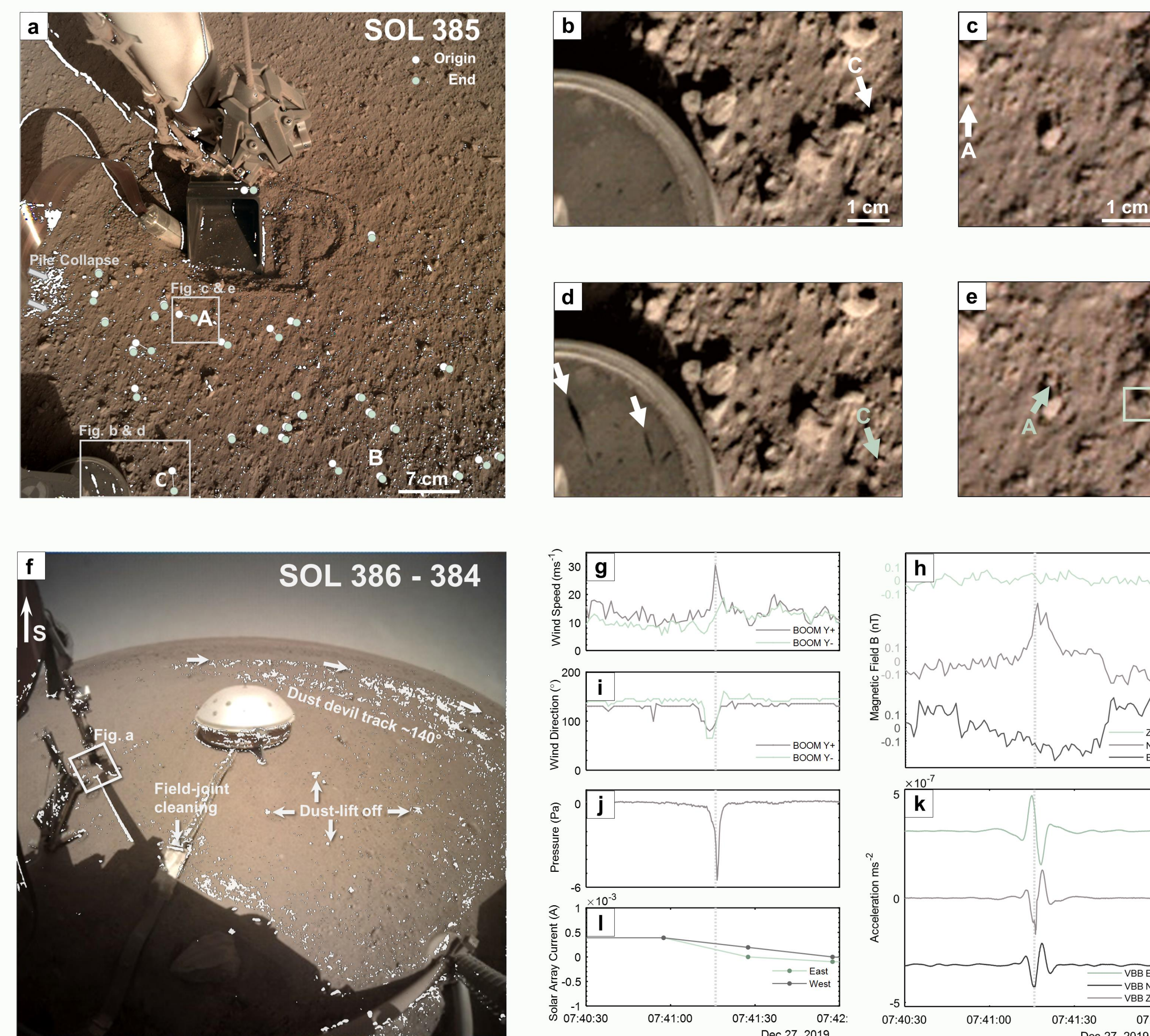
Overall, our observations suggest that surface material is mobilised infrequently and for short durations, likely due to high tangential velocities from passing vortices, enhanced by increased ambient wind speeds. Below is a compilation of all changes, correlated to increased vortex activity, measured as the daily number of - a proxy of atmospheric activity over the 400-sol investigation.



6. Surface creep, dust removal and saltation

Images from S362-S364 and S385 show episodes of surface creep by particles of diameters up to 2 mm and 3 mm , respectively. IDC image differencing for S383-S385 (Fig a), suggests widespread subtle changes across the FOV with numerous dark spots on pebbles, indicative of dust-coating removal. A pile of regolith collapsed parallel to the direction of particle creep. 'Splash' marks are seen in the dust coating of the HP3's footpad, revealing the original surface and oriented in approximately the same direction as nearby particle creep and wind direction, suggesting saltation occurred (Fig. b, d). Lack of striation paths on the ground could indicate that larger grains reptated (Fig c,e).

ICC differencing shows cleaning of the field joint and dust coating removals from protruding rocks (Fig. f). The widest DD track observed so far aligns to the dominant wind direction ($\sim 130^\circ$, SE-NW). Map projection suggests a width of at least 4 m , with the edge approaching within 1 m of SEIS. The ground acceleration validates the selection of this vortex, suggesting a direction of travel from SE-NW, or the inverse. Estimates show a peak wind speed at 30.5 ms^{-1} and $\Delta P = 6 \text{ Pa}$ was recorded on S385. Surface creep for S364 shows a maximum of 31.6 ms^{-1} , with a $\Delta P = 3.5 \text{ Pa}$.



Magnetic Signatures

For all near-lander observations discussed so far, with evident episodes of dust entrainment during a vortex's passage, there are associated excursions in B, indicating a response to the vortex passing. Assuming these are not caused by solar array current changes and/or panel motion, or other sources, they may provide a probe of the electric charge present on dust grains mobilised by the vortex. Such a charge could be produced by, for example, triboelectric charging (Eden et al., 1973).

Conclusion

Convective vortices appear to be the primary channel for dust entrainment at the InSight landing site, as well as drivers for sporadic motion such as surface creep of grains $d < 3 \text{ mm}$, and likely saltation. All episodic aeolian changes are correlated with excursions in both seismic and magnetic signals as might be expected from vortex-induced ground movement and charged-particle motion, respectively.

